Diatom delta C-13, delta N-15, and C/N since the Last Glacial Maximum in the Southern Ocean: Potential impact of Species Composition

Hélène Jacot Des Combes, Oliver Esper, Christina L. de La Rocha, Andrea Abelmann, Rainer Gersonde, Ruth Yam, Aldo Shemesh

Diatom $\delta^{13}C$, $\delta^{15}N$, and C/N since the Last Glacial Maximum in the Southern Ocean: Potential impact of Species Composition

H. Jacot Des Combes,[1,2] O. Esper,[1] C. L. De La Rocha,[1,3] A. Abelmann,[1] R. Gersonde,[1] R. Yam,[2] and A. Shemesh[2]

Received 8 January 2008; revised 29 July 2008; accepted 13 August 2008; published 7 November 2008.

[1] Measurements of $\delta^{13}C$, $\delta^{15}N$, and C/N on diatom-bound organic matter were made over the Holocene and Last Glacial Maximum (LGM) from three sediment cores in the Southern Ocean, one each from the Atlantic, Indian, and Pacific sectors. The site in the Scotia Sea (Atlantic sector) differed considerably from the other two sites by having markedly lower $\delta^{13}C$, more variable $\delta^{15}N$ and C/N ratios, and a sedimentary diatom assemblage that was never dominated by *Fragilariopsis kerguelensis*. Although environmental parameters certainly have a strong impact on the isotope ratios, $\delta^{13}C$ is also correlated to the proportion of *F. kerguelensis* in the three cores investigated here ($r^2 = 0.8$). Extreme values of $\delta^{13}C$, $\delta^{15}N$, and C/N at the Last Glacial Maximum were also related to the abundance of winter stages of *Eucampia antarctica*. These results suggest that diatom specific isotope records should be interpreted in conjunction with information on the species composition of the samples.

Citation: Jacot Des Combes, H., O. Esper, C. L. De La Rocha, A. Abelmann, R. Gersonde, R. Yam, and A. Shemesh (2008), Diatom $\delta^{13}C$, $\delta^{15}N$, and C/N since the Last Glacial Maximum in the Southern Ocean: Potential impact of Species Composition, *Paleoceanography*, *23*, PA4209, doi:10.1029/2008PA001589.

1. Introduction

[2] The carbon and nitrogen isotopic composition ($\delta^{13}C$ and $\delta^{15}N$) and C/N ratio of diatom-bound organic matter are commonly used to reconstruct oceanographic processes that contribute to variations in atmospheric CO_2 over glacial-interglacial cycles. High values of $\delta^{15}N$ at the Last Glacial Maximum (LGM) suggest that the percent draw down of nitrate by phytoplankton was higher during glacials without a corresponding maximum in net primary production and that therefore surface water stratification contributed to the lower concentration of CO_2 in the atmosphere [*François et al.*, 1997; *Sigman and Boyle*, 2000]. Peaks in the C/N ratio at the LGM have been hypothesized to reflect nitrogen limitation of phytoplankton growth [*Crosta and Shemesh*, 2002], supporting the nitrogen isotope results. $\delta^{13}C$, while controlled by a complex set of biological and physical factors, has been interpreted as indicating changes in primary production, sea surface temperature, and sea ice coverage [*Crosta and Shemesh*, 2002; *Schneider-Mor et al.*, 2005].

[3] Although these are sophisticated interpretations, the controls on the carbon and nitrogen isotopic composition and elemental ratio of diatom-bound organic matter are not well understood [*De La Rocha*, 2006]. This organic material is presumed to be part of the diatom cell wall and the template for biomineralization [*Swift and Wheeler*, 1992; *Kröger et al.*, 1999], entombed within the silica and protected from diagenesis [*Singer and Shemesh*, 1995; *Sigman et al.*, 1999]. This material has not been well characterized and there is no strong sense for how variable its composition is between species or among members of the same species growing under different conditions (although it is well known that diatom cell wall material as a whole, in terms of the types and relative proportions of its sugars and amino acids, is quite variable from species to species and with environmental conditions [*Hecky et al.*, 1973]). In addition, the culturing studies that have been carried out on C and N isotopic fractionation by diatoms have focused on the isotopic composition of the whole cell (i.e., including the cytoplasm in addition to the cell wall) and not specifically the isotopic composition of the material occluded within the matrix of the silica [*Hinga et al.*, 1994; *Laws et al.*, 1995; *Needoba et al.*, 2003].

[4] Organic material from within the silica contains serine, glycine, and tyrosine-rich proteins [*Swift and Wheeler*, 1992; *Kröger et al.*, 1999, 2002]. Proteins associated with the diatom frustule have been classed into three types (frustulins, silaffins, and pleuralins) that are to varying degrees peripheral to, embedded in, or attached to the cell wall [*Kröger et al.*, 1999, 2002]. The cell wall also contains polysaccharides [*Hecky et al.*, 1973; *Granum et al.*, 2002], although it is not clear to what extent polysaccharides are present in the material entombed within the silica. The previously observed variability in the C/N ratio of diatom-bound organic matter (i.e., between 3 and 11 mol mol^{-1}) [*Crosta et al.*, 2002] suggests that there may be not only a significant amount of polysaccharide within the silica matrix but that the relative amount of it is quite variable.

[5] Although comparison of Holocene and LGM diatom valves from one site in the Southern Ocean suggested little

[1] Alfred Wegener Institute for Marine and Polar Research, Bremerhaven, Germany.
[2] Department of Environmental Sciences and Energy Research, Weizmann Institute of Science, Rehovot, Israel.
[3] Now at Laboratoire des Sciences de l'Environnement Marin, Institut Universitaire Européen de la Mer, Université de Bretagne Occidentale, Brest, France.

0883-8305/08/2008PA001589$12.00

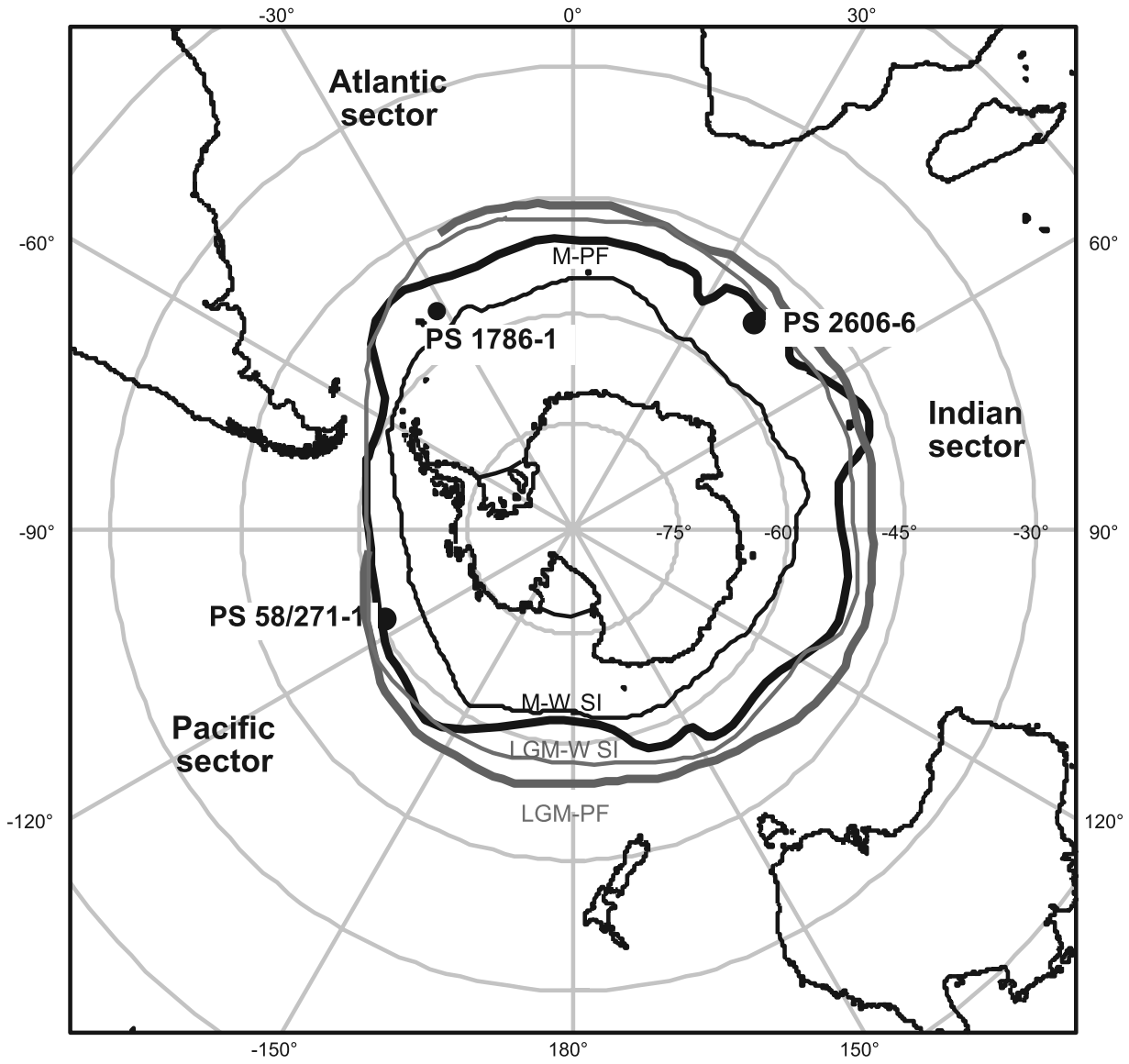

Figure 1. Location of the three sediment core sites in the Southern Ocean. Modern Polar Front (M-PF) have been placed according to *Belkin and Gordon* [1996], and modern winter sea ice extent (M-WSI) is defined as that having more than 15% coverage in September (1979–1999). The placement of the M-WSI boundary follows *Comiso* [2003]. Epilog LGM Polar Front (LGM-PF) and Epilog LGM winter sea ice extent (LGM-WSI) have been placed following *Gersonde et al.* [2005].

change in their amino acid composition over time [*Shemesh et al.*, 1993], if the composition of the occluded organic matter is variable enough, this variability will play a role in the downcore variations in carbon and nitrogen isotopes and C/N ratios observed in diatom-bound organic matter. For example, proteins tend to be enriched in ^{15}N relative to cell material as a whole [*Werner and Schmidt*, 2002]. Amino acids, of which proteins are constructed, can differ from one another in δ^{15}N by as much as 10‰ and in their δ^{13}C by as much as 20‰ [*Macko et al.*, 1987].

[6] The interpretation of the isotopic and major element composition of diatom-bound organic matter in sediment cores presumes consistency to the signatures produced at different times and places by all particular diatom species. This is a topic that has not been adequately addressed. Here we present a comparison of diatom-bound δ^{15}N, δ^{13}C, and C/N ratio records from 3 sediment cores from different settings in the Southern Ocean, south of the present-day Polar Front. By coupling these records with data on the diatom species abundances, a first assessment of the robustness of the proxies over geographic locality and diatom species composition has been made.

2. Material and Methods

2.1. Sediment Cores

[7] One cm samples covering the Holocene and Last Glacial Maximum (LGM: 23–19 cal ka BP [*Mix et al.*,

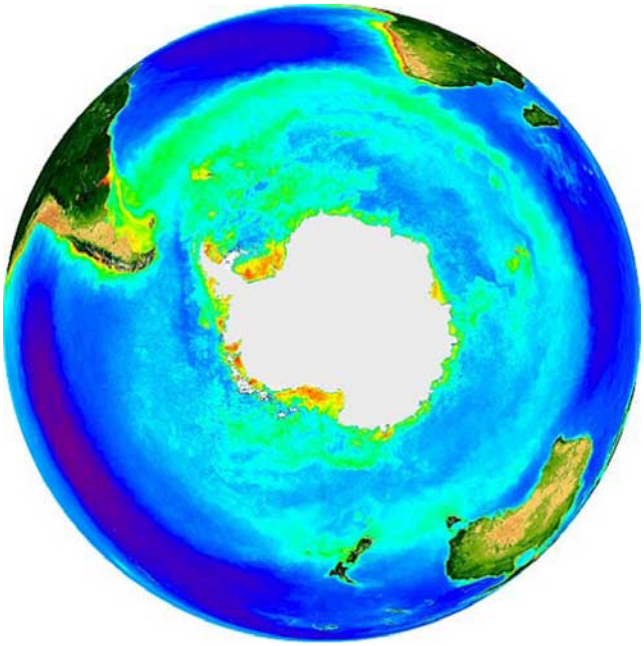

Figure 2. Distribution of chlorophyll in the Southern Ocean during austral summer. Note the greater and more uniform abundance of chlorophyll in the Atlantic sector (downwind of Patagonia), in coastal regions, and in other areas near landmasses which can serve as sources of Fe. Image courtesy of the SeaWiFS Project, NASA/GSFC and GeoEYE.

2001]) were taken at 10 cm intervals from 3 sediment cores in the Southern Ocean (Figure 1), core PS 2606-6 (53.23°S, 40.80°E, 2545 mbsl) from the western Indian sector, core PS 58/271-1 (61.24°S, 116.05°W, 5214 mbsl) from the eastern Pacific sector, and core PS 1786-1 (54.92°S, 31.72°W, 5862 mbsl) from the Scotia Sea, western Atlantic sector. All three core positions are located south of the present-day Antarctic Polar Front (APF) and were chosen to represent different environmental conditions during both the Holocene and the last glacial, especially in term of sea ice coverage. The site from the Scotia Sea (Atlantic sector) is the site which is closest to the sea ice edge and currently has the highest amount of dust [*Wagener et al.*, 2008] and chlorophyll (Figure 2) compared to the sites from the Indian and Pacific sectors.

[8] The stratigraphy of these cores is based on AMS-^{14}C measurements, with 4–6 control points in each of the cores (Table 1 and Figure 3). The AMS-^{14}C measurements were made on the acid insoluble of base soluble humic fraction extracted from the sediment. Samples were prepared and analyzed at the Leibniz Labor für Alterbestimmung und Isotopenforschung in Kiel (Germany). ^{14}C ages were converted to calendar years using CALIB4.2 [*Stuiver et al.*, 1998] after applying a reservoir age of 810, 750 and 840 years at the Indian, Pacific, and Atlantic sites, respectively [*Bard*, 1988]. The age of the samples located between the control points was obtained by linear interpolation, and the resulting age model was refined by the use of stratigraphic markers like variations in the abundance of *Eucampia antarctica* [*Gersonde et al.*, 2003].

2.2. Separation and Cleaning of Samples

[9] Diatom opal was separated from bulk sediment using a series of physical separation and chemical cleaning steps [*Singer and Shemesh*, 1995]. First, the <20 μm size fraction (the one most predominantly diatom and also the one most devoid of opal produced by radiolarians) was isolated from the bulk sediment through sieving and sonication. Carbonate and bulk organic matter were removed via reaction with a 50:50 (vol vol^{-1}) solution of concentrated HCl and 30% H_2O_2 at room temperature. Diatoms were separated from mineral grains using the heavy liquid, sodium polytungstate. Any remaining organic matter external to the diatom opal was removed in a second digestion in the acidified peroxide solution for 2 h at 60°C. Slides were made of each cleaned sample and checked to ensure that radiolarian opal and mineral silicate grains had been eliminated. That these procedures sufficiently cleaned extraneous organic matter from the samples was demonstrated by measurements of weight percent carbon in these samples of 0.2 to 0.4%.

2.3. Isotopic Analysis and Measurement of C/N Ratios

[10] The carbon (δ^{13}C) and nitrogen (δ^{15}N) isotopic composition, and the C and N content of organic matter

Table 1. Sample Depth, Laboratory ID, Carbon Source, and Ages of the Samples Analyzed for AMS-^{14}C Measurements

Core	Depth (cmbsf)	Laboratory ID	C Source	^{14}C Age (ka BP)	Error (ka)	Reservoir Age (ka)	Reservoir Corrected ^{14}C Age (cal ka BP)
PS 1786-1	2–3.5 + 6–7.5	KIA16766H	humic acid	2.725	±0.025	0.84	1.895
PS 1786-1	71.5–75	KIA16767H	humic acid	5.655	±0.040	0.84	5.581
PS 1786-1	121.5–124.5	KIA16768H[a]	humic acid	9.355	±0.070	0.84	9.534
PS 1786-1	181–184	KIA16770H[a]	humic acid	16.275	+0.305/−0.290	0.84	18.327
PS 2606-6	126–130	KIA16759AH	humic acid	6.210	±0.130	0.81	6.209
PS 2606-6	226–230	KIA16760AH	humic acid	7.110	±0.110	0.81	7.236
PS 2606-6	273–277	KIA16761AH	humic acid	7.700	+0.170/−0.160	0.81	7.826
PS 2606-6	316–320	KIA23790H	humic acid	9.860	±0.060	0.81	10.263
PS 2606-6	425–429	KIA16764H	humic acid	16.650	±0.100	0.81	18.793
PS 2606-6	516–520	KIA16765H	humic acid	20.340	±0.210	0.81	23.039
PS 58/271-1	14–17	KIA16755H	humic acid	6.150	±0.070	0.75	6.209
PS 58/271-1	113–117	KIA16756H	humic acid	9.570	±0.100	0.75	9.833
PS 58/271-1	212–217	KIA16757H[a]	humic acid	14.480	+0.185/−0.180	0.75	16.365
PS 58/271-1	271–275	KIA23793H	humic acid	19.690	+0.170/−0.160	0.75	22.360

[a]Samples where the ^{14}C ages were obtained by averaging values from two analyses.

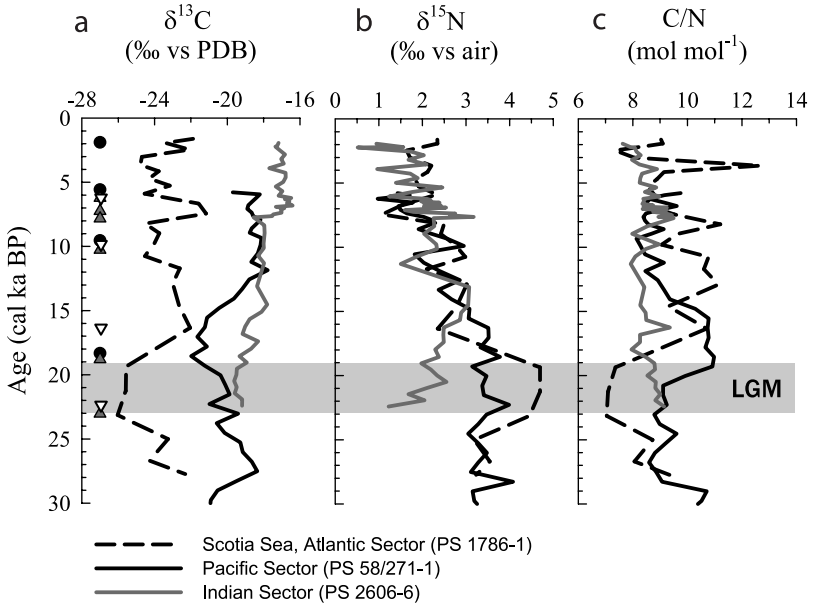

Figure 3. Opal-based records from three sites in the Southern Ocean. Core PS 1786-1, Scotia Sea (dashed line); core PS 58/271-1, Pacific sector (solid black line); and core PS 2606-6, Indian sector (solid grey line). These records extend to the last glacial. (a) δ^{13}C record, (b) δ^{15}N record, and (c) C/N ratio record. The Epilog LGM [*Mix et al.*, 2001] is indicated as a shaded band. The symbols located along the age scale on the left indicate the control points of the ^{14}C age calibration. They are black circles for core PS 1786-1, white upside down triangles for core PS 58/271-1, and grey triangles for core PS 2606-1. These data are available online in the Pangaea database (http://www.pangaea.de/).

encased within the cleaned diatom opal were measured at the Weizmann Institute of Science. Measurements were made using a Carlo Erba EA1110 elemental analyzer in line with a Finnigan MAT 252 stable isotope ratio mass spectrometer. Isotopic and abundance data for carbon and nitrogen were measured from the same runs via peak jumping. At least two replicates were measured for each sample. δ^{13}C values are reported versus peedee belemnite (PDB) and δ^{15}N is reported versus air. The %C and %N data were combined to establish the C/N (mol mol^{-1}) ratio of the opal-bound organic matter. Elemental analyzer runs were checked for internal consistency using several calibrated laboratory standards (acetanilide, glycine, and cellulose). The mean 1σ standard deviation was 0.17‰ and 0.24‰ for δ^{13}C and δ^{15}N, respectively. %C and %N measurements had a mean standard deviation of 0.0007% and 0.005% respectively.

2.4. Diatom Species Counts

[11] Given the impossibility of making counts on the cleaned, sonicated <20 μm size fraction (which contained a considerable proportion of fragmented diatom frustules), quantitative slides for diatom species counts on the whole assemblage were prepared and performed following the description by *Gersonde and Zielinski* [2000]. For each sample, a known volume of decarbonated and peroxide-treated sediment was evenly dispersed in a gelatin solution, pipetted onto a glass slide, and allowed to dry at room temperature. Once dry, samples were fixed into resin (Meltmount) at 160°C. At least 400 valves were counted in traverses over the slide with a Zeiss microscope at a magnification of 1000 x. The taxonomy of *Zielinski* [1993] was followed. The sea ice diatom group consisted of the species: *Fragilariopsis cylindrus, F. curta*, *F. ritscheri, F. obliquecostata, F. sublineares,* and *Actinocyclus actinochilus*. The ''other diatoms'' group was made up of 35 different species, including *Thalassiosira lengitinosa*, *T. gracilis*, *F. separanda, Thalassiothrix antarctica,* and *Azpeitia tabularis var. tabularis.*

[12] Although the sieved, sonicated, and cleaned material could not also be quantitatively counted, slides of this material were inspected and changes observed in the species composition of the whole diatom assemblage from core PS 1786−1 in the Atlantic sector were also qualitatively present in the isotopically analyzed material. This is not surprising given that the bulk of the diatom opal wound up in the sonicated and cleaned <20 μm opal fraction.

3. Results

[13] There is little to no overlap in the δ^{13}C values in the three cores at any given time over the last 32 ka. δ^{13}C ranges from −26.0 to −21.2‰ in the Scotia Sea (Atlantic sector) core (PS1786−1), from −22.0 to −17.8‰ in the Pacific sector core (PS 58/271−1), and from −19.6 to −16.4‰ in the Indian sector core (PS 2606−6) (Figure 3a). The Scotia Sea core also differs from the other two by showing strong variations during the Holocene. As a result,

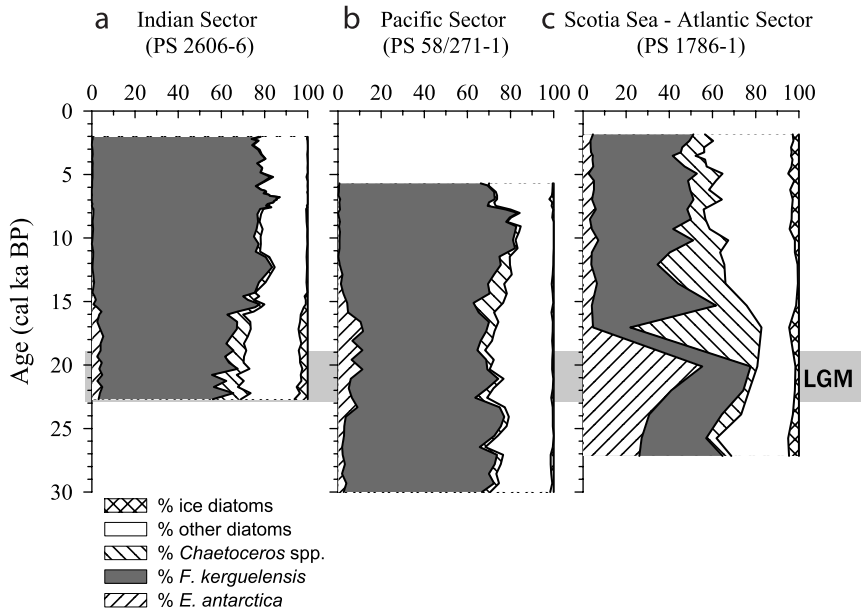

Figure 4. Abundance of selected diatom species at the three sites from the Southern Ocean. The percent of *Fragilariopsis kerguelensis*, *Eucampia antarctica*, *Chaetoceros* spp, ice diatoms, and the remaining species (''other diatoms'') are shown for (a) the Indian sector, (b) the Pacific sector, and (c) the Scotia Sea. *E. antarctica* and *Chaetoceros* spp. fractions are both predominantly made up of heavily silicified winter stages/resting spores. The Epilog LGM [*Mix et al.*, 2001] is indicated as a shaded band. These data are available online in the Pangaea database (http://www.pangaea.de/).

although the $\delta^{13}C$ values are lower during the LGM than during the Holocene, the offset between the LGM values and the lowest Holocene values is relatively small. In the Pacific sector, the $\delta^{13}C$ values are at a minimum just after the LGM (Figure 3a).

[14] $\delta^{15}N$ ranges from +0.5 to +3.2‰ in the Indian sector core, from +1.0 to +4.1‰ in the Pacific sector core, and from +1.1 to +4.7‰ in the Scotia Sea core (Figure 3b). In contrast to $\delta^{13}C$, the $\delta^{15}N$ values from the three cores are comparable during the Holocene, but they diverge distinctly before 14 cal ka BP. There is a generally downward trend in $\delta^{15}N$ from the LGM toward the present day.

[15] As with $\delta^{15}N$, C/N profiles of the three cores are roughly coincident, although the Atlantic core shows a greater range of variation than do the other two cores (Figure 3c). C/N in the Indian, Pacific, and Atlantic cores range from 7.6 to 9.5 (mol mol^{-1}), from 8.1 to 10.9 (mol mol^{-1}), and from 6.8 to 12.9 (mol mol^{-1}), respectively. The Indian sector core shows similar values during the both last glacial and the Holocene, whereas in the Scotia Sea (Atlantic sector) core, lowest values during the LGM are followed by a sharp rise. The Pacific sector core shows low values during the Holocene and before and during the first half of the LGM, and maximum values at the end of and shortly after the LGM (Figure 3c). At both the Pacific sector and the Scotia Sea sites, the C/N ratio is correlated to the amount of carbon in the samples ($r^2 = 0.45$, $p < 0.01$ and $r^2 = 0.51$, $p < 0.01$, respectively), but not to the amount of nitrogen. No such relationships are observed in the Indian sector core.

[16] In terms of bulk diatom species composition of the cores as a whole, *Fragilariopsis kerguelensis* is the most common species, generally making up 40 to 80% of the species assemblage (Figure 4). In the Scotia Sea core, the next 2 most abundant groups are *Chaetoceros* spp. and *E. antarctica*, peaking at 60 and 55%, respectively. In the other cores, however, these groups never represent more than 12% of the assemblage each. Up to one third of the diatoms in the cores are neither *F. kerguelensis*, *Chaetoceros* spp., nor *E. antarctica*, falling instead into the category of ''other diatoms.'' Sea ice diatoms never exist in great number in any of the cores.

[17] In the Indian sector (Figure 4a), the species composition is dominated by *F. kerguelensis* (at ca. 70–80%), but with slightly greater abundances of *E. antarctica* and *Chaetoceros* spp. occurring between 23 and 15 cal ka BP. In the Pacific core (Figure 4b), the relative abundance of *F. kerguelensis*, *Chaetoceros* spp., and *E. antarctica* is fairly steady over the time interval considered, except for a minor peak in *E. antarctica* between 22 and 18 cal ka BP. The Scotia Sea core is the only one not clearly dominated by *F. kerguelensis* (Figure 4c). The abundance of *F. kerguelensis* is never more than 58% in this core and plummets down to 17 to 30% in the interval between 17 and 27 cal ka BP, in part to accommodate peaks in *Chaetoceros* spp. and

E. antarctica. This last peak is part of a drastic shift in *E. antarctica* abundances from glacial values up to 30% to Holocene values around 5%. The glacial peak may be partly related to stronger opal dissolution occurring during the interval between 17 and 27 cal ka BP.

4. Discussion

4.1. Regional Differences in Diatom $\delta^{13}C$

[18] Of the three cores presented here, only the Scotia Sea core shows peak values in diatom $\delta^{13}C$ during the Holocene and distinctly minimum values at the LGM, as has been seen in several other cores from the Southern Ocean, including ODP Site 1094 which spans seven glacial-interglacial transitions [*Shemesh et al.*, 1993, 2002; *Singer and Shemesh*, 1995; *Rosenthal et al.*, 2000; *Crosta and Shemesh*, 2002; *Crosta et al.*, 2005; *Schneider-Mor et al.*, 2005]. The most striking feature of the $\delta^{13}C$, $\delta^{15}N$, and C/N records, when taken together, is that the $\delta^{15}N$ and C/N records are both roughly coincident between Indian sector, Pacific sector, and Scotia Sea sites while $\delta^{13}C$ can differ between two sites by as much as 8‰ (Figure 3).

[19] That there might be regional variations in $\delta^{13}C$ is not new. In bulk samples of particulate organic matter (POM) from the Southern Ocean, geographic variability in $\delta^{13}C \geq 8‰$ has been previously observed, with, just as seen here, more negative values occurring in the Atlantic Sector [*Rau et al.*, 1982, 1989, 1997; *Freeman and Hayes*, 1992; *Goericke and Fry*, 1994]. Other published records of diatom-bound $\delta^{13}C$ also show offsets between the various Southern Ocean sectors [*Rosenthal et al.*, 2000; *Crosta and Shemesh*, 2002].

[20] These differences in the $\delta^{13}C$ of POM and diatom-bound organic matter between Southern Ocean sectors, and the particularly negative values of the Atlantic Sector, have never been satisfactorily explained. It is not that there is much regional variation in the $\delta^{13}C$ of dissolved inorganic carbon (DIC) of surface waters. Some differences exist [*Kroopnick*, 1985; *Rau et al.*, 1989], but nothing on the order of the several permil necessary to explain the POM and diatom-bound organic matter data.

[21] Likewise sea surface temperatures (SSTs) are unlikely to be making a substantial contribution to the isotopic variations. Temperature has only a minor influence on isotope fractionation between gaseous and dissolved CO_2 [*Vogel et al.*, 1970] and anyway large regional variations in the $\delta^{13}C$ of dissolved CO_2 have already been ruled out [*Rau et al.*, 1982, 1989]. True, temperature influences dissolved CO_2 solubility and therefore concentrations [*Rau et al.*, 1989; *Goericke and Fry*, 1994] and it affects phytoplankton growth rates and the expression of carbon isotope fractionation [*Rau et al.*, 1992, 1996; *François et al.*, 1993; *Goericke and Fry*, 1994; *Laws et al.*, 1995; *Dehairs et al.*, 1997] in ways that might translate into variability in the $\delta^{13}C$ of organic matter. But SSTs reconstructed via diatom-based transfer functions for the three sediment core sites reported here indicate little variation in temperature between these sites. The less than 1°C differences suggested cannot really account for offsets in the $\delta^{13}C$ of diatom-bound organic matter of several permil.

[22] Another possibility is the presence of sea ice, which, by inhibiting ventilation of CO_2 from upwelled deep waters, could induce a decrease in the $\delta^{13}C$ of DIC in surface waters [*Shemesh et al.*, 1993; *Stephens and Keeling*, 2000; *Crosta and Shemesh*, 2002]. Increased ice coverage could have also influenced carbon and nitrogen utilization by diatoms in certain areas, leading to regional differences in $\delta^{15}N$ and $\delta^{13}C$. The abundance of sea ice diatoms present in the sedimentary assemblage of diatoms (Figure 4) suggests that the core site in the Scotia Sea (Figure 1), the one with the significantly lower $\delta^{13}C$ values (Figure 3), was the only one to have winter sea ice during the Holocene (O. Esper, personal communication, 2007). However, as with SST, it is difficult to relate the low $\delta^{13}C$ values entirely to the extended sea ice presence at the Scotia Sea site. Models indicate that even substantially expanded coverage of the Southern Ocean with sea ice in winter would drive down the $\delta^{13}C$ of surface water DIC by less than 1‰ [*Stephens and Keeling*, 2000], far less than the up to 8‰ difference observed between the Scotia Sea core and the others. Similar conclusions have been drawn on the basis of planktonic foraminiferan $\delta^{13}C$ [*Shemesh et al.*, 1993].

[23] If physical parameters cannot explain the regional patterns in POM and diatom-bound $\delta^{13}C$, the patterns must be biological in origin, most likely tied to disparity in overall rates of primary production or in the way that primary production is carried out. The $\delta^{13}C$ of phytoplankton ($\delta^{13}C_{phyto}$) is set during the photosynthetic production of organic matter and is related to the isotopic composition of dissolved CO_2 ($\delta^{13}C_{ce}$), isotope fractionation associated with the diffusion of CO_2 into the phytoplankton cell (ε_d), isotope fractionation during the capture of CO_2 by the enzyme, Rubisco (ε_f), and the balance between intracellular and extracellular concentrations of dissolved CO_2 (C_i and C_e, respectively):

$$\delta^{13}C_{phyto} = \delta^{13}C_{ce} - \varepsilon_d - (\varepsilon_f - \varepsilon_d)(c_i/c_e) \qquad (1)$$

[*Laws et al.*, 1995; *Rau et al.*, 1996, 1997; *Hofmann et al.*, 2000]. Because of this multiplicity of factors, phytoplankton $\delta^{13}C$ cannot be precisely or quantitatively used as a proxy for primary production or CO_2 concentrations [*Laws et al.*, 1995]. In addition, different forms and subtle differences in the same forms of Rubisco mean that different phytoplankton species have different values of ε_f [*Scott et al.*, 2007]. Phytoplankton growth rates, cell size, cell shape, and the potential use of carbon concentrating mechanisms all affect the balance between c_i and c_e, allowing for greater or less extent of the carbon isotope fractionation associated with CO_2 fixation by Rubisco to be expressed (see equation (1)) [*Laws et al.*, 1995; *Rau et al.*, 1996, 1997, 2001].

[24] In other words, low rates of carbon fixation in combination with high concentrations of dissolved CO_2 in surface waters would allow for a more full expression of the potentially −25 to −28‰ isotope discrimination of the carbon-fixing enzyme, Rubisco, resulting in the production of organic matter of lower $\delta^{13}C$ than under conditions of higher growth rates or lower concentrations of dissolved CO_2 [*Laws et al.*, 1995; *Rau et al.*, 1996]. Similarly, low

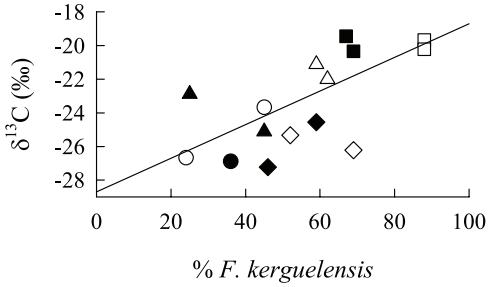

Figure 5. The $\delta^{13}C$ of POC from the euphotic zone in the water column during the SOIREE Fe fertilization experiment in the Southern Ocean versus the abundance of *F. kerguelensis* in the samples. Filled symbols indicate samples from Fe-fertilized waters, and unfilled symbols represent samples from unfertilized waters. Diamonds represent the >200 μm size fraction, circles represent the 70–200 μm size fraction, squares represent the 20–70 μm size fraction, and triangles represent the 5–20 μm size fraction. Data are from *Trull and Armand* [2001]. The regression shown is $y = -0.10x - 28.7$; $r^2 = 0.44$; $n = 14$; $p = 0.01$.

rates of carbon fixation relative to the resupply of dissolved CO_2 into surface waters would prevent a rise in the $\delta^{13}C$ of the dissolved CO_2 reservoir (and thus of the subsequently produced organic matter) through Rayleigh distillation as CO_2 concentrations were drawn down.

[25] Unfortunately, here again, the lower $\delta^{13}C$ values of the Scotia Sea in the Atlantic sector of the Southern Ocean cannot be explained. If anything, this sector exhibits higher overall levels and rates of primary production than the other two sectors, exactly the opposite of what is needed to explain the $\delta^{13}C$ of POM and diatom-bound organic matter. Standing stocks of chlorophyll during productive times of the year are notably higher here (Figure 2), implying higher rates of primary production.

[26] The higher concentrations of chlorophyll are likely related to the input of dust from Patagonia into the Atlantic sector, especially in the west [*Mahowald et al.*, 1999; *Wagener et al.*, 2008], and thus of the often-limiting micronutrient, iron; large parts of the Pacific and Indian sectors, too distantly removed from any such dust source, are likely to be significantly more iron limited than the Atlantic sector. Iron enrichment experiments in the Southern Ocean indicate that inputs of iron to surface waters here shifts the structure of the phytoplankton community toward domination by large diatoms (*Fragilariopsis*, *Thalassiothrix*, and *Odontella* spp.), and increases the rates of growth and carbon uptake by these diatoms [*Gall et al.*, 2001a, 2001b; *Hoffmann et al.*, 2006; *Assmy et al.*, 2007], all things that should drive the $\delta^{13}C$ of both bulk POM and diatom organic matter up and not down. Because all of the organic matter within a diatom cell (including that occluded within the opal) is produced during photosynthesis, there should be a direct link between bulk cell and opal bound organic matter values.

[27] If temperature, the $\delta^{13}C$ of dissolved CO_2, Fe availability, and overall patterns of primary production cannot explain the differences in the $\delta^{13}C$ of POM and diatom-bound organic matter between sectors of the Southern Ocean and the low values found in the Scotia Sea, what remains as the main controlling factor of the $\delta^{13}C$ of organic matter in the Southern Ocean in both modern times and over glacial-interglacial cycles? One possibility is for the $\delta^{13}C$ differences to be related to the species of diatoms preserved in the sediments. The size, surface to volume ratio, growth rate, and specifics of the carbon fixing enzyme, Rubisco, for each species leave room for differences in the $\delta^{13}C$ of different phytoplankton growing under different conditions [*Laws et al.*, 1995; *Rau et al.*, 1996, 1997, 2001; *Popp et al.*, 1998; *Hofmann et al.*, 2000; *Scott et al.*, 2007]. It may very well be that the higher $\delta^{13}C$ values of cores from the Pacific and Indian sectors are tied to the solid predominance of *F. kerguelensis* in the sediments there, something which is not true in core PS 1786–1 from the Scotia Sea where *F. kerguelensis* makes up only between 10 and 45% of the diatom assemblage (Figure 4). Correlation between the carbon isotopic composition of particulate organic carbon (POC) and the relative abundance of *F. kerguelensis* in samples can, after all, be seen in published data from the water column (Figure 5), so it would not be too surprising to see it also in the sediments.

4.2. Influence of Species Composition on Diatom-Bound $\delta^{13}C$ and $\delta^{15}N$

[28] Despite grave differences in cleaning and analytical methods employed in obtaining $\delta^{13}C$ and $\delta^{15}N$ from fossil diatoms in various studies [e.g., *Crosta and Shemesh*, 2002; *Crosta et al.*, 2002, 2005; *Robinson et al.*, 2004, 2005], most studies of diatom-bound organic matter in Southern Ocean sediments (from south of the present-day Antarctic Polar Front) report an increase in $\delta^{13}C$ [*Shemesh et al.*, 1993, 2002; *De La Rocha et al.*, 1998; *Rosenthal et al.*, 2000; *Crosta and Shemesh*, 2002; *Crosta et al.*, 2005; *Schneider-Mor et al.*, 2005; *Singer and Shemesh*, 1995] and a decrease in $\delta^{15}N$ [*François et al.*, 1992, 1997; *Crosta and Shemesh*, 2002; *Shemesh et al.*, 2002; *Crosta et al.*, 2005; *Robinson et al.*, 2005; *Schneider-Mor et al.*, 2005] between LGM and the Holocene. The situation here is more complex. Although an increase in $\delta^{13}C$ is observed between the last glacial and the Holocene, its intensity varies from site to site, as does the exact timing of the lowest $\delta^{13}C$ values (Figure 3). Regarding $\delta^{15}N$, the generally observed decrease between LGM and the Holocene is not observed in the Indian Ocean core, although the record does not span the entire LGM interval (Figure 3).

[29] The hypotheses put forward to explain the trends are tied to nutrient cycling and primary production. The LGM maximum in $\delta^{15}N$ has been ascribed to nitrate concentrations being drawn down to relatively low levels, because of biological utilization, and, likewise, the minimum in $\delta^{13}C$ has been related to the balance between CO_2 uptake and availability [*François et al.*, 1992, 1997; *Singer and Shemesh*, 1995; *De La Rocha et al.*, 1998; *Rosenthal et al.*, 2000; *Crosta and Shemesh*, 2002; *Shemesh et al.*, 2002; *Robinson et al.*, 2004, 2005; *Crosta et al.*, 2005; *Schneider-Mor et al.*, 2005]. Given the importance of understanding what is going on with the biological pump

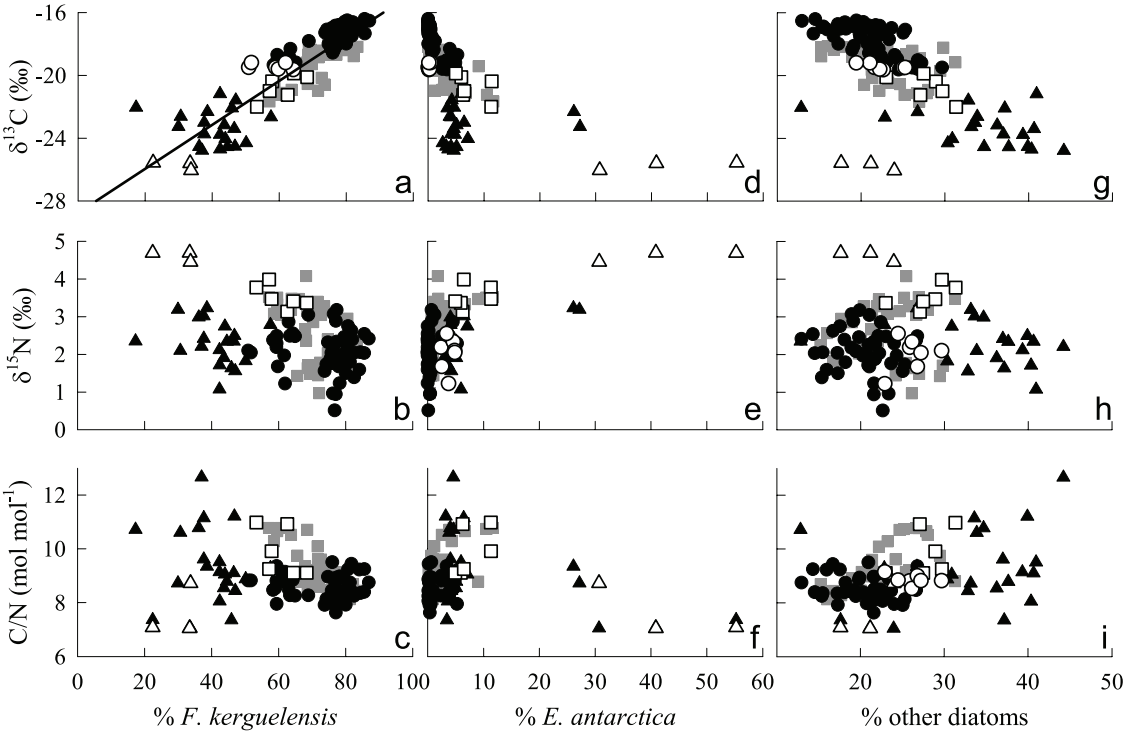

Figure 6. Variation of isotopes and C/N with abundances of (a–c) *F. kerguelensis*, (d–f) *E. antarctica*, and (g–i) "other diatoms" in the sedimentary diatom assemblage. Black triangles correspond to the Scotia Sea (Atlantic sector), gray squares correspond to the Pacific sector, and black circles correspond to the Indian sector. Samples from the LGM are white. The significant regression lines shown in Figure 6a are for the data set as a whole ($y = 0.14x - 28.75$; $r^2 = 0.80$; $n = 129$; $p = 0.01$).

in the glacial Southern Ocean, and that nutrient utilization proxies based on diatom opal are the most direct way of assessing this, it is worth considering if there is an ecological component to the signal. Can the observed LGM extrema in diatom $\delta^{13}C$ and $\delta^{15}N$ be the result of changes in the species composition of the sediments analyzed? This is a possibility which was not reported in any previous studies, none of which made direct, quantitative comparisons between species abundances and isotopic values [*Rosenthal et al.*, 2000; *Crosta et al.*, 2002].

[30] That species abundances have an influence on sedimentary diatom $\delta^{13}C$ values is strongly suggested by the data reported here (although it should be again pointed out that the isotope measurements were made on the <20 μm fraction and the species counts were carried on the bulk assemblage). In the Scotia Sea core (Figure 3), the only one to show the expected extrema at the LGM, the three samples with notably high $\delta^{15}N$ and notably low $\delta^{13}C$ (and the lowest values of C/N) fall between 18 and 24 cal ka BP. This interval corresponds to a huge peak (more than 50%) in the amount of *E. antarctica* in the sediments (Figure 4), and, conversely, to the lowest *F. kerguelensis* abundances (10 to 30%). This peak in *E. antarctica* abundance is related to a strong dissolution event that resulted in the preferential preservation of heavily silicified diatom species, like *E. antarctica.*

[31] A plot of $\delta^{13}C$ against the abundance of *F. kerguelensis* reveals a strong correlation between the two (Figure 6a). The relationship is significant for all three cores taken together ($y = 0.14x - 28.75$; $r^2 = 0.80$; $n = 129$; $p = 0.01$), and for the Pacific sector core ($y = 0.12x - 27.87$; $r^2 = 0.60$; $n = 42$; $p = 0.01$) and Indian sector core ($y = 0.09x - 24.47$; $r^2 = 0.73$; $n = 52$; $p = 0.01$) taken individually. Interestingly, the relationship between $\delta^{13}C$ and *F. kerguelensis* only fails to be significant in the Scotia Sea ($y = 0.03x - 24.75$; $r^2 = 0.03$; $n = 42$; $p > 0.05$), the site exhibiting the lowest and most variable values of $\delta^{13}C$ and lowest and more variable abundances of *F. kerguelensis*.

[32] Although it may be that the species composition of diatoms in the sediments is tightly correlated to some environmental change responsible for the shifts in $\delta^{13}C$, it is more likely that changes in the species composition are directly responsible for the downcore $\delta^{13}C$ signal and for the lower values in the Scotia Sea. In areas where *F. kerguelensis* overwhelmingly dominates the sedimentary assemblage (e.g., the Pacific and Indian sectors; Figure 4), the sedimentary diatom $\delta^{13}C$ appears to primarily reflect the balance between the abundance of *F. kerguelensis* and the rest of the diatom species taken as a whole. Alternatively, it may be that the signal represents mainly a balance between *F. kerguelensis* and the fraction remaining that is not *E. antarctica* nor *Chaetoceros* spp. (i.e., the "other diatoms"),

as in the Pacific and Indian sector cores it is this "other diatom" fraction that makes up the only other large component of the sedimentary assemblage.

[33] In areas, such as the Scotia Sea, where *F. kerguelensis* abundances are lower and no one fraction overwhelmingly dominates the sedimentary assemblage, the control of $\delta^{13}C$ is more complex. While the lower values of $\delta^{13}C$ here are most easily explained by the predominance of species other than *F. kerguelensis*, changes in the values cannot just be explained by the degree of absence of *F. kerguelensis*. The three other major diatom species and species groups, *E. antarctica*, *Chaetoceros* spp., and "other diatoms," each contribute significantly and variably to the sedimentary assemblage and must have average $\delta^{13}C$ values that are relatively different from one another. For example, just as plots of $\delta^{13}C$ versus *F. kerguelensis* hint at high values of $\delta^{13}C$ for this species (Figure 6a), plots against *E. antarctica* abundance (Figure 6d) suggest low values for *E. antarctica*. The resulting total diatom $\delta^{13}C$ value thus follows no one species' abundance directly.

[34] The relationship between $\delta^{15}N$ (or C/N ratios) and species composition is not as strong as with $\delta^{13}C$ (Figures 6b, 6e, and 6h). Although the highest $\delta^{15}N$ values in the Atlantic and Pacific sector cores correspond to the lowest abundances of *F. kerguelensis*, there is only a significant correlation between $\delta^{15}N$ and *F. kerguelensis* abundance in the Pacific sector core ($y = -0.06x + 6.80$; $r^2 = 0.32$; $n = 42$; $p = 0.05$). The Pacific site is also the only one to show a significant relationship between C/N ratio and *F. kerguelensis* abundance ($y = -0.08x + 15.10$; $r^2 = 0.55$; $n = 42$; $p = 0.01$). This may be because $\delta^{15}N$ and C/N are not as strongly variable between diatoms species. Or this may represent analytical artifacts associated with measuring the low levels of N trapped within the diatom silica [*Robinson et al.*, 2004].

[35] It appears that *E. antarctica* tends to have high values of $\delta^{15}N$, as shown by the high values in sediment cores when *E. antarctica* abundances reach 10% or higher (Figure 6e). *E. antarctica* may also have relatively low values of $\delta^{13}C$ (Figure 6d) and low C/N ratios (Figure 6f), as shown by the extreme LGM values on these plots. No strong sense of the isotopic or elemental composition of the *Chaetoceros* spp. fraction can be discerned (data not shown). Not much can be said about the average isotopic or elemental composition of the "other diatom" fraction, either, save that, by virtue of being the second component of what is essentially a two-component mixture (Figures 6a and 6g), the $\delta^{13}C$ of the "other diatom" fraction must be lower than that of *F. kerguelensis*.

[36] If we are to successfully interpret paleoceanographic records of diatom $\delta^{13}C$ and $\delta^{15}N$, and they are, as they appear to be, linked to the species being analyzed, we need to understand where these species differences are coming from. While Figure 6 shows this is certainly an issue for $\delta^{13}C$, the correspondence between the abundance of *E. antarctica* and high $\delta^{15}N$ values at the LGM also demand consideration. The high $\delta^{13}C$ values of *F. kerguelensis* are most likely physiological, related to factors affecting carbon uptake, c.f. [*Rau et al.*, 1997] and may not reflect environmental conditions. This diatom dominates the open ocean species assemblage in the water column [*Smetacek et al.*, 2004; *Assmy et al.*, 2007] and occurs predominately in areas where the dissolved silicon to nitrate ratio in the surface ocean is high [*Abelmann et al.*, 2006]. Its growth may be spurred on briefly by inputs of Fe, as seen in the Fe fertilization experiment, EisenEx [*Assmy et al.*, 2007], but its low abundance in the most Fe-fertilized and productive sector of the Southern Ocean suggests that it is not a species necessarily recording signals tied to high levels of primary production and nutrient utilization [*Abelmann et al.*, 2006].

[37] While the high diatom $\delta^{15}N$ values observed at the LGM may be reflecting heavy consumption of the nutrient nitrate, a cause associated with the increased abundance of *E. antarctica* in the sediments at this time cannot be ruled out (Figure 6e). First, it is already known that there are species-specific fractionation factors for nitrate utilization [*Needoba et al.*, 2003]. Second, *E. antarctica* is, as well as *Chaetoceros* spp., a fast growing, weakly silicified species, and its normal vegetative cells are not preserved in sediments. The *E. antarctica* cells that are found are winter stages, a heavily silicified form produced as a response to decreasing daylight [*Fryxell and Prasad*, 1990]. Thus the signal of nutrient "utilization" recorded by this species may correspond to the nutrient availability at the end of the bloom season, as opposed to giving a signal integrated across the entire growing season.

[38] The species composition of diatoms in the sediments, even in the Southern Ocean, is variable between sectors, with latitude, and back through time, making the possibility of species shifts contributing to downcore isotopic records is a very real one. Although it is not completely clear whether these shifts are related solely to environmental changes or the result of the dissolution of the more weakly silicified species, this is something that must be investigated in more detail in order to improve paleoceanographic interpretation of $\delta^{13}C$ and $\delta^{15}N$. Although progress is being made on the separation of more specific opal fractions out of sediments via laminar flow techniques [e.g., *Rings et al.*, 2004], we are some ways off from being able to effectively separate out monospecific diatom samples. Until that time, it is imperative that data on the abundance of diatom species in the samples analyzed be given alongside the records of diatom-bound $\delta^{13}C$ and $\delta^{15}N$.

4.3. Composition of the Diatom-Bound Organic Matter, as Defined by C/N

[39] Although the diatom cell wall as a whole contains a significant amount of polysaccharides, especially on the external surface [*Hecky et al.*, 1973], analyses of the organic material entombed within the silica of the cell wall reveals that it is largely made of proteins and polyamines [*Swift and Wheeler*, 1992; *Kröger et al.*, 1999, 2000]. The C/N ratio of the proteins from marine plankton averages 3.8 mol mol^{-1} and shows minimal variability between species and location [*Hedges et al.*, 2002]. Given this, it is surprising that the C/N ratio of diatom-bound organic matter is much higher and relatively variable, falling generally between 6 and 14 mol mol^{-1} (Figure 3) [*Sigman et al.*, 1999; *Crosta and Shemesh*,

2002; *Crosta et al.*, 2005; *Schneider-Mor et al.*, 2005]. C/N values as high as 14 mol mol^{-1} require that the organic matter being analyzed contain a significant proportion of carbohydrate or lipid, things which contain essentially no nitrogen.

[40] This raises questions about exactly what the fossil diatom organic matter being analyzed is. Does it represent a pure and intact fraction of the organic template for silicification and therefore imply that there is a lot of polysaccharide in this material? Or is it that measurements of diatom-bound organic matter are contaminated by external material strongly attached to the diatom frustule, that cleaning methods partially degrade the entombed organic matter, or that the cell wall material is not in fact protected from diagenesis as surmised? Or is it related to the difficulty of measuring diatom-bound N (and therefore C/N) on such small samples (resulting in large errors relative to the variability in %N) and the possibility for contamination from atmospheric N during analysis [*Robinson et al.*, 2004]?

[41] In the cores analyzed here, C/N ratios do not appear to be linked with the $\delta^{15}N$ of the samples. In none of the cores looked at (nor in all of them as a whole) is there a significant slope to the relationship between C/N and $\delta^{15}N$. There is, however a significant correlation between $\delta^{13}C$ and C/N ratios in the Pacific sector core ($y = -1.22x - 8.14$; $r^2 = 0.78$, $n = 42$; $p = 0.01$). This may indicate that the percentage of polysaccharide or lipid in the organic matter analyzed is fueling some of the observed variation in $\delta^{13}C$, adding further complexity to the interpretation of $\delta^{13}C$ in diatom-bound organic matter.

5. Conclusions

[42] Although $\delta^{15}N$, in particular, and $\delta^{13}C$ and the C/N ratio of organic matter occluded within sedimentary diatoms are important paleoceanographic proxies, it appears that the interpretation of these proxies is not perfectly simple. Variations in the C/N ratio of the diatom bound organic matter show that the organic matter varies in composition from sample to sample. In all three cores reported here, $\delta^{13}C$ values were linked to diatom species abundances, in particular to the abundance of *F. kerguelensis*. It also appears that extreme values at the LGM in $\delta^{15}N$ that have previously been ascribed to nutrient drawdown might be related to the increased incidence of *E. antarctica* winter stages. These data suggest that combined publication of records of diatom-bound $\delta^{13}C$ and $\delta^{15}N$ and of abundance of diatom species in the samples analyzed would help interpretation of the isotope composition of opal-bound organic matter.

[43] **Acknowledgments.** Thanks are owed to P. Assmy and D. Wolf-Gladrow for helpful discussions and to G. Feldman for permission to use the SEAWIFS globe. We also want to thank the technicians from A. Shemesh's lab at the Weizmann Institute in Rehovot for their help and support in the lab. This work was supported by GIF grant G-649-154.8/1999, EPICA-MIS (contract 3868) within the 6th EU Framework Programme, and the DFG Research Center, Ocean Margins. G. Rau and one anonymous reviewer provided instructive comments on this manuscript.

References

Abelmann, A., R. Gersonde, G. Cortese, G. Kuhn, and V. Smetacek (2006), Extensive phytoplankton blooms in the Atlantic sector of the glacial Southern Ocean, *Paleoceanography, 21, PA1013, doi:10.1029/2005PA001199.*

Assmy, P., J. Henjes, C. Klaas, and V. Smetacek (2007), Mechanisms determining species dominance in a phytoplankton bloom induced by the iron fertilization experiment EisenEx in the Southern Ocean, *Deep Sea Res., Part I*, *54*, 340–362, doi:10.1016/j.dsr.2006.12.005.

Bard, E. (1988), Correction of accelerator mass spectrometry ^{14}C ages measured in planktonic foraminifera: Paleoceanographic implications, *Paleoceanography*, *3*, 635–645, doi:10.1029/PA003i006p00635.

Belkin, I. M., and A. L. Gordon (1996), Southern ocean fronts from the Greenwich meridian to Tasmania, *J. Geophys. Res.*, *101*, 3675–3696, doi:10.1029/95JC02750.

Comiso, J. C. (2003), Large-scale characteristics and variability of the global sea ice cover, in *Sea Ice: An Introduction to Its Physics, Chemistry, Biology and Geology*, edited by D. N. Thomas and G. S. Diekmann, pp. 112–142, Blackwell, Oxford, U. K.

Crosta, X., and A. Shemesh (2002), Reconciling down core anticorrelation of diatom carbon and nitrogen isotopic ratios from the Southern Ocean, *Paleoceanography*, *17*(1), 1010, doi:10.1029/2000PA000565.

Crosta, X., A. Shemesh, M.-E. Salvignac, H. Gildor, and R. Yam (2002), Late quaternary variations of elemental ratios (C/Si and N/Si) in diatom-bound organic matter from the Southern Ocean, *Deep Sea Res., Part II*, *49*, 1939–1952, doi:10.1016/S0967-0645(02)00019-X.

Crosta, X., A. Shemesh, J. Etourneau, R. Yam, I. Billy, and J.-J. Pichon (2005), Nutrient cycling in the Indian sector of the Southern Ocean over the last 500,000 years, *Global Biogeochem. Cycles*, *19*, GB3007, doi:10.1029/2004GB002344.

Dehairs, F., E. Kopczynska, P. Nielsen, C. Lancelot, D. C. E. Bakker, W. Koeve, and L. Goeyens (1997), $\delta^{13}C$ of Southern Ocean suspended organic matter during spring and early summer: Regional and temporal variability, *Deep Sea Res., Part II*, *44*, 129–142, doi:10.1016/S0967-0645(96)00073-2.

De La Rocha, C. L. (2006), Opal-based proxies of paleoenvironmental conditions, *Global Biogeochem. Cycles*, *20*, GB4S09, doi:10.1029/2005GB002664.

De La Rocha, C. L., M. A. Brzezinski, M. J. DeNiro, and A. Shemesh (1998), Silicon-isotope composition of diatoms as an indicator of past oceanic change, *Nature*, *395*, 680–683, doi:10.1038/27174.

François, R., M. A. Altabet, and L. H. Burckle (1992), Glacial to interglacial changes in surface nitrate utilization in the Indian sector of the Southern Ocean as recorded by sediment $\delta^{15}N$, *Paleoceanography*, *7*, 589–606, doi:10.1029/92PA01573.

François, R., M. A. Altabet, R. Goericke, D. C. McCorkle, C. Brunet, and A. Poisson (1993), Changes in the $\delta^{13}C$ of surface water particulate organic matter across the subtropical convergence in the SW Indian Ocean, *Global Biogeochem. Cycles*, *7*, 627–644, doi:10.1029/93GB01277.

François, R., M. A. Altabet, E.-F. Yu, D. M. Sigman, M. P. Bacon, M. Frank, G. Bohrman, G. Bareille, and L. D. Labeyrie (1997), Contribution of Southern Ocean surface-water stratification to low atmospheric CO_2 concentrations during the last glacial period, *Nature*, *389*, 929–935, doi:10.1038/40073.

Freeman, K. H., and J. M. Hayes (1992), Fractionation of carbon isotopes by phytoplankton and estimates of ancient CO_2 levels, *Global Biogeochem. Cycles*, *6*, 185–198, doi:10.1029/92GB00190.

Fryxell, G. A., and A. K. S. K. Prasad (1990), *Eucampia antactica* var. *recta* (Mangin) stat. nov. (Biddulphiaceae, Bacillariophyceae): Life stages at the Weddell Sea ice edge, *Phycologia*, *29*, 27–38.

Gall, M. P., P. W. Boyd, J. Hall, K. A. Safi, and H. Chang (2001a), Phytoplankton processes. Part 1: Community structure during the Southern Ocean Iron Release Experiment (SOIREE), *Deep Sea Res., Part II*, *48*, 2551–2570, doi:10.1016/S0967-0645(01)00008-X.

Gall, M. P., R. Strzepek, M. Maldonado, and P. W. Boyd (2001b), Phytoplankton processes. Part 2: Rates of primary production and factors controlling algal growth during the Southern Ocean Iron Release Experiment (SOIREE), *Deep Sea Res., Part II*, *48*, 2571–2590, doi:10.1016/S0967-0645(01)00009-1.

Gersonde, R., and U. Zielinski (2000), The reconstruction of late Quaternary Antarctic sea-ice distribution—The use of diatoms as a proxy for sea-ice, *Palaeogeogr. Palaeoclimatol. Palaeoecol.*, *162*, 263–286, doi:10.1016/S0031-0182(00)00131-0.

Gersonde, R., et al. (2003), Last glacial sea surface temperatures and sea-ice extent in the Southern Ocean (Atlantic-Indian sector): A multiproxy approach, *Paleoceanography*, *18*(3), 1061, doi:10.1029/2002PA000809.

Gersonde, R., X. Crosta, A. Abelmann, and L. Armand (2005), Sea-surface temperature and sea ice distribution of the Southern Ocean at the EPILOG Last Glacial Maximum—A circum-Antarctic view based on siliceous microfossil records, *Quat. Sci. Rev.*, *24*, 869–896, doi:10.1016/j.quascirev.2004.07.015.

Goericke, R., and B. Fry (1994), Variations of marine plankton $\delta^{13}C$ with latitude, temperature, and dissolved CO_2 in the world ocean, *Global Biogeochem. Cycles*, *8*, 85–90, doi:10.1029/93GB03272.

Granum, E., S. Kirkvold, and S. M. Mykelstad (2002), Cellular and extracellular production of carbohydrates and amino acids by the marine diatom *Skeletonema costatum*: Diel variations and effects of N depletion, *Mar. Ecol. Prog. Ser.*, *242*, 83–94, doi:10.3354/meps242083.

Hecky, R. E., K. Mopper, P. Kilham, and E. T. Degens (1973), The amino acid and sugar composition of diatom cell-walls, *Mar. Biol. Berlin*, *19*, 323–331, doi:10.1007/BF00348902.

Hedges, J. I., J. A. Baldock, Y. Gélinas, C. Lee, M. L. Peterson, and S. G. Wakeham (2002), The biochemical and elemental composition of marine plankton: A NMR perspective, *Mar. Chem.*, *78*, 47–63, doi:10.1016/S0304-4203(02)00009-9.

Hinga, K. R., M. A. Arthur, M. E. Q. Pilson, and D. Whitaker (1994), Carbon isotope fractionation by marine phytoplankton in culture: The effects of CO_2 concentration, pH, temperature, and species, *Global Biogeochem. Cycles*, *8*, 91–102, doi:10.1029/93GB03393.

Hoffmann, L. J., I. Peeken, K. Lochte, P. Assmy, and M. Veldhuis (2006), Different reactions of Southern Ocean phytoplankton size classes to iron fertilization, *Limnol. Oceanogr.*, *51*, 1217–1229.

Hofmann, M., D. A. Wolf-Gladrow, T. Takahashi, S. C. Sutherland, K. D. Six, and E. Maier-Reimer (2000), Stable carbon isotope distribution of particulate organic matter in the ocean: A model study, *Mar. Chem.*, *72*, 131–150, doi:10.1016/S0304-4203(00)00078-5.

Kröger, N., R. Deutzmann, and M. Sumper (1999), Polycationic peptides from diatom biosilica that direct silica nanosphere formation, *Science*, *286*, 1129–1132, doi:10.1126/science.286.5442.1129.

Kröger, N., R. Deutzmann, C. Bergsdorf, and M. Sumper (2000), Species-specific polyamines from diatoms control silica morphology, *Proc. Natl. Acad. Sci. U. S. A.*, *97*, 14,133–14,138, doi:10.1073/pnas.260496497.

Kröger, N., S. Lorenz, E. Brunner, and M. Sumper (2002), Self-assembly of highly phosphorylated silaffins and their function in biosilica morphogenesis, *Science*, *298*, 584–586, doi:10.1126/science.1076221.

Kroopnick, P. M. (1985), The distribution of ^{13}C of $\sum CO_2$ in the world oceans, *Deep Sea Res.*, *32*, 57–84, doi:10.1016/0198-0149(85)90017-2.

Laws, E. A., B. N. Popp, R. R. Bidigare, M. C. Kennicutt, and S. A. Macko (1995), Dependence of phytoplankton carbon isotopic composition on growth rate and $[CO_2]_{aq}$: Theoretical considerations and experimental results, *Geochim. Cosmochim. Acta*, *59*, 1131–1138, doi:10.1016/0016-7037(95)00030-4.

Macko, S. A., M. L. Fogel, P. E. Hare, and T. C. Hoering (1987), Isotopic fractionation of nitrogen and carbon in the synthesis of amino acids by microorganisms, *Chem. Geol.*, *65*, 79–92, doi:10.1016/0009-2541(87)90196-3.

Mahowald, N., K. Kohfeld, M. Hansson, Y. Balkanski, S. P. Harrison, I. C. Prentice, M. Schulz, and H. Rodhe (1999), Dust sources and deposition during the last glacial maximum and current climate: A comparison of model results with paleodata from ice cores and marine sediments, *J. Geophys. Res.*, *104*, 15,895–15,916, doi:10.1029/1999JD900084.

Mix, A. C., E. Bard, and R. Schneider (2001), Environmental processes of the ice age: Land, oceans, glaciers (EPILOG), *Quat. Sci. Rev.*, *20*, 627–658, doi:10.1016/S0277-3791(00)00145-1.

Needoba, J. A., N. A. Waser, P. J. Harrison, and S. E. Calvert (2003), Nitrogen isotope fractionation in 12 species of marine phytoplankton during growth on nitrate, *Mar. Ecol. Prog. Ser.*, *255*, 81–91, doi:10.3354/meps255081.

Popp, B. N., E. A. Laws, R. R. Bidigare, J. E. Dore, K. L. Hanson, and S. G. Wakeham (1998), Effect of phytoplankton cell geometry on carbon isotopic fractionation, *Geochim. Cosmochim. Acta*, *62*, 69–77, doi:10.1016/S0016-7037(97)00333-5.

Rau, G. H., R. E. Sweeney, and I. R. Kaplan (1982), Plankton $^{13}C/^{12}C$ ratio changes with latitude: Differences between northern and southern oceans, *Deep Sea Res. A*, *29*, 1035–1039.

Rau, G. H., T. Takahashi, and D. J. Des Marais (1989), Latitudinal variations in plankton $\delta^{13}C$: Implications for CO_2 and productivity in past oceans, *Nature*, *341*, 516–518, doi:10.1038/341516a0.

Rau, G. H., T. Takahashi, D. J. Des Marais, D. J. Repeta, and J. H. Martin (1992), The relationship between organic matter $\delta^{13}C$ and $[CO_2aq]$ in ocean surface waters: Data from a JGOFS site in the northeast Atlantic Ocean and a model, *Geochim. Cosmochim. Acta*, *56*, 1413–1419, doi:10.1016/0016-7037(92)90073-R.

Rau, G. H., U. Riebesell, and D. Wolf-Gladrow (1996), A model of photosynthetic ^{13}C fractionation by marine phytoplankton based on diffusive molecular CO_2 uptake, *Mar. Ecol. Prog. Ser.*, *133*, 275–285, doi:10.3354/meps133275.

Rau, G. H., U. Riebesell, and D. Wolf-Gladrow (1997), CO_{2aq}-dependent photosynthetic ^{13}C fractionation in the ocean: A model versus measurements, *Global Biogeochem. Cycles*, *11*, 267–278, doi:10.1029/97GB00328.

Rau, G. H., F. P. Chavez, and G. E. Friederich (2001), Plankton $^{13}C/^{12}C$ variations in Monterey Bay, California: Evidence of non-diffusive inorganic carbon uptake by phytoplankton in an upwelling environment, *Deep Sea Res., Part I*, *48*, 79–94, doi:10.1016/S0967-0637(00)00039-X.

Rings, A., A. Lücke, and G. H. Schleser (2004), A new method for the quantitative separation of diatom frustules from lake sediments, *Limnol. Oceanogr. Methods*, *2*, 25–34.

Robinson, R. S., B. G. Brunelle, and D. M. Sigman (2004), Revisiting nutrient utilization in the glacial Antarctic: Evidence from a new method for diatom-bound N isotope analysis, *Paleoceanography*, *19*, PA3001, doi:10.1029/2003PA000996.

Robinson, R. S., D. M. Sigman, P. J. DiFiore, M. M. Rohde, T. A. Mashiotta, and D. W. Lea (2005), Diatom-bound $^{15}N/^{14}N$: New support for enhanced nutrient consumption in the ice age subantarctic, *Paleoceanography*, *20*, PA3003, doi:10.1029/2004PA001114.

Rosenthal, Y., M. Dahan, and A. Shemesh (2000), Southern Ocean contribution to glacial-interglacial changes of atmospheric pCO_2: An assessment of carbon isotope records in diatoms, *Paleoceanography*, *15*, 65–75, doi:10.1029/1999PA000369.

Schneider-Mor, A., R. Yam, C. Bianchi, M. Kunz-Pirrung, R. Gersonde, and A. Shemesh (2005), Diatom stable isotopes, sea ice presence and sea surface temperature records of the past 640 ka in the Atlantic sector of the Southern Ocean, *Geophys. Res. Lett.*, *32*, L10704, doi:10.1029/2005GL022543.

Scott, K. M., M. Henn-Sax, T. L. Harmer, D. L. Longo, C. H. Frame, and C. M. Cavanaugh (2007), Kinetic isotope effect and biochemical characterization of form IA RubisCO from the marine cyanobacterium *Prochlorococcus marinus* MIT9313, *Limnol. Oceanogr.*, *52*, 2199–2204.

Shemesh, A., S. A. Macko, C. D. Charles, and G. H. Rau (1993), Isotopic evidence for reduced productivity in the Glacial Southern Ocean, *Science*, *262*, 407–410, doi:10.1126/science.262.5132.407.

Shemesh, A., D. Hodell, X. Crosta, S. Kanfoush, C. Charles, and T. Guilderson (2002), Sequence of events during the last deglaciation in Southern Ocean sediments and Antarctic ice cores, *Paleoceanography*, *17*(4), 1056, doi:10.1029/2000PA000599.

Sigman, D. M., and E. A. Boyle (2000), Glacial/interglacial variations in atmospheric carbon dioxide, *Nature*, *407*, 859–869, doi:10.1038/35038000.

Sigman, D. M., M. A. Altabet, R. François, D. C. McCorkle, and J.-F. Gaillard (1999), The isotopic composition of diatom-bound nitrogen in Southern Ocean sediments, *Paleoceanography*, *14*, 118–134, doi:10.1029/1998PA900018.

Singer, A. J., and A. Shemesh (1995), Climatically linked carbon isotope variation during the past 430,000 years in Southern Ocean sediments, *Paleoceanography*, *10*, 171–177, doi:10.1029/94PA03319.

Smetacek, V., P. Assmy, and J. Henjes (2004), The role of grazing in structuring Southern Ocean pelagic ecosystems and biogeochemical cycles, *Antarct. Sci.*, *16*, 541–558, doi:10.1017/S0954102004002317.

Stephens, B. B., and R. F. Keeling (2000), The influence of Antarctic sea ice on glacial-interglacial CO_2 variations, *Nature*, *404*, 171–174, doi:10.1038/35004556.

Stuiver, M., P. J. Reimer, E. Bard, J. W. Beck, G. S. Burr, K. A. Hughen, B. Kromer, G. McCormac, J. van der Plicht, and M. Spurk (1998), INTCAL98 radiocarbon age calibration, 24,000–0 cal BP, *Radiocarbon*, *40*, 1041–1083.

Swift, D. M., and A. P. Wheeler (1992), Evidence of an organic matrix from diatom biosilica, *J. Phycol.*, *28*, 202–290, doi:10.1111/j.0022-3646.1992.00202.x.

Trull, T. W., and L. Armand (2001), Insights into Southern Ocean carbon export from the $\delta^{13}C$ of particles and dissolved inorganic carbon during SOIREE iron release experiment, *Deep Sea Res., Part II*, *48*, 2655–2680, doi:10.1016/S0967-0645(01)00013-3.

Vogel, J. C., P. M. Grootes, and W. G. Mook (1970), Isotopic fractionation between gaseous and dissolved carbon dioxide, *Z. Phys.*, *230*, 225–238, doi:10.1007/BF01394688.

Wagener, T., C. Guieu, R. Losno, S. Bonnet, and N. Mahowald (2008), Revisiting atmospheric dust export to the Southern Hemisphere ocean: Biogeochemical implications, *Global Biogeo-*

chem. Cycles, *22*, GB2006, doi:10.1029/2007GB002984.

Werner, R. A., and H.-L. Schmidt (2002), The in vivo nitrogen isotope discrimination among organic plant compounds, *Phytochemistry*, *61*, 465–484, doi:10.1016/S0031-9422(02)00204-2.

Zielinski, U. (1993), Quantitative Bestimmung von Paläoumweltparametern des Antarktichen Oberflächenwassers im Spätquartär anhand von Transferfunktionen mit Diatomeen, *Ber. Polar Forsch. 126*, 148 pp., AWI Bremerhaven, Bremerhaven, Germany.

A. Abelmann, R. Gersonde, H. Jacot Des Combes, and O. Esper, Alfred Wegener Institute for Marine and Polar Research, Am Alten Hafen 26, D-27568 Bremerhaven, Germany. (helene.jacot.descombes@awi.de)

C. L. De La Rocha, Laboratoire des Sciences de l'Environnement Marin, Institut Universitaire Européen de la Mer, Université de Bretagne Occidentale, F-29238 Brest, France. (christina.delarocha@univ-brest.fr)

A. Shemesh and R. Yam, Department of Environmental Sciences and Energy Research, Weizmann Institute of Science, Rehovot 76100, Israel.